

## Developments in a model to describe low-frequency electrical polarization of rocks

Carlos A. Dias\*

### ABSTRACT

The author reworks his total current conductivity function introduced in a previous paper, related to electrical polarization of rocks in the frequency range of 1 MHz to  $10^{-3}$  Hz. The original five parameters in this function are replaced by new ones, which from the beginning have clear petrophysical and electrochemical meanings and well-defined ranges of variation. Some classical models are derived as particular cases of it. The main existing models proposed to describe induced polarization (IP) are analyzed, and most of them are grouped together under a common circuit analog representation and a respective generating function. A circuit analog is assigned to each model. The multi-Cole–Cole model circuit analog reveals intrinsic constraints involving the

values of its circuit elements. Because of these constraint relations and the relaxation times ratio ( $\tau_1/\tau_2$ )—usually many orders of magnitude from unity—the model has no physical validation to represent single-phase material systems (in the sense of the polarization). The performance and analysis of the various models to describe a few well-selected experimental data show that only two of the models, the multi-Cole–Cole and Dias models, can provide a function structure capable of fitting these data. This fact, the associated petrophysical interpretation consistency, and the basic characteristics of these two models, such as the way they were derived (empirically, the former; phenomenologically, the latter) and the number of coefficients in the function (directly related to the degree of ambiguity of their determination), make the author's model attractive and promising.

### INTRODUCTION

Electrical polarization in rocks containing disseminated metallic and/or ion-exchange-capable minerals in contact with ionic solutions filling their pore spaces has been studied by several researchers in exploration geophysics since 1946 (Brant, 1959). This phenomenon has been observed in the frequency domain in the range of 1 MHz to  $10^{-3}$  Hz under an applied harmonic electric field (time dependence  $e^{i\omega t}$ ) and, correspondingly, in the time domain.

This type of electrical polarization is understood to be primarily caused by the movement of free and bound ions in the neighborhood of the interface between the ionic solution and the solid conductive (metallic) or ion-exchange-competent (clay, zeolite, and some organic) particles. The flow of ions and their possible chemical reactions in the liquid phase result in an ohmic (induced) and a diffusion-produced conduction through a transport current, eventually combined with chemically generated displacement currents and, in parallel, capacitive effects resulting from electrical oscillations of a fixed layer of positive

ions adsorbed on the particle surface and of the outer limit of the excess electrical charge concentration in the ionic solution (Madden and Marshall, 1959a,b; Fraser et al., 1964; Madden and Cantwell, 1967; Ward and Fraser, 1967; Dias, 1968, 1972; Bockris and Reddy, 1970; Angoran and Madden, 1977; Klein et al., 1984; Olhoeft, 1985).

In the initial decades of experimental research on this subject, the a priori assumption of real quantities for the bulk electrical parameters of a rock sample, conductivity ( $\sigma$ ) and dielectric permittivity ( $\epsilon$ ), when this kind of polarization is present led to unexpectedly high values of the dielectric constant, defined as  $K = \epsilon/\epsilon_0$ , where  $\epsilon_0 = 8.854 \times 10^{-12}$  F/m is the vacuum value of  $\epsilon$  (Evjen, 1948; Keller, 1959; Keller and Licastro, 1959; Ward and Fraser, 1967; Scott et al., 1967). This disconcerting situation caused much concern about the quality of the measurements; however, the effort to improve laboratory instrumentation lowered the old values of  $K$  by no more than one order of magnitude (Scott et al., 1967; Collet and Katsube, 1973). The work of Dias (1968), partly published in Dias (1972), clarifies basic points on this matter—points that make up the fundamentals

Manuscript received by the Editor April 8, 1996; revised manuscript received September 16, 1999.

\*North Fluminense State University, LENEP/UENF, Rod. Amaral Peixoto, Km 164, Imboacica-Macaé CEP 27.973-030, RJ, Brazil. E-mail: dias@lenep.uenf.br.

© 2000 Society of Exploration Geophysicists. All rights reserved.

of our original model. To clarify my assumptions, their limitations, and the possible consequences for my later model, I summarize these points as follows.

- 1) I recognize simultaneous dispersion of both conductivity and dielectric permittivity, each exhibiting in-phase and quadrature components. Their simultaneous characterization as complex quantities implies that there is no way to separate their individual real and imaginary parts on an experimental basis. Fuller and Ward (1970) also address this point.
- 2) This rock polarization is represented by a single constitutive electrical parameter, defined as total current conductivity, in the context of Maxwell equations written for the average values of fields and parameters for a core sample of rock. I did this because most of this type of polarization is produced by the movement of free moving charge carriers.
- 3) I describe most of the reliable experimental data available at the time, using the same type of (complex) conductivity functions. These data consist of spectra of conductivity amplitude (Fraser et al., 1964) and independent measurements of  $\sigma$  and  $K$ , both of which are taken a priori as real quantities (Scott et al., 1967).
- 4) Both kinds of rock polarization are described and associated with either disseminated metallics (electrode polarization) or clay particles (membrane polarization) using the same type of conductivity function. The covered frequency intervals in the first case were  $10^{-1}$  to  $10^3$  Hz; in the second case they were  $10^2$  to  $10^6$  Hz. More recently, I have found that this type of function gives, without exception, a good description of electrode polarization over the whole spectrum but has limitations confronting a given set of experimental data for membrane polarization at frequencies below 1 Hz.
- 5) I demonstrate that an equivalent circuit analog, defined as the fundamental circuit, corresponding to a parallel combination of a free ionic path with another term exhibiting the full effect of polarization (associated with a single interface of a metal, clay, or similar material with an electrolyte) can generate the desired function representation for conductivity. This occurs in spite of many series and/or parallel combinations of resistors and/or fundamental circuits contributing to the bulk behavior of a given rock sample (see Appendix A). I assume that the fundamental circuits involved differ from each other by just a scale factor. From a physical standpoint, this approach is equivalent to saying that the fundamental circuit represents an average unit cell of the electrical behavior of the polarizable medium and that the medium is therefore composed of many of those units in such a way that it leaves unchanged the function representation for the conductivity. Seeing a core sample of rock as a network system, the fundamental circuit could be considered as the simplest equivalent circuit analog that can generate the same admittance function representation as the network. The fundamental point in this view is that the model generates an invariant type of function representation for the conductivity; the internal arrangements of the network elements and the pure geometric factors related to pore dimensions account for only the coefficients

entering the function. The determination of these coefficients is ultimately made by matching the experimental data using the formal conductivity function. The fundamental circuit analog proposed by Dias (1968, 1972) is reproduced in Figure 1.

- 6) The fundamental circuit selected is comprised of two parallel combined basic components, taken within the realm of linearity in the frequency domain. The first component is a simple resistor that describes the pure ohmic conduction associated to a free ionic path. Its regular presence in the unit cell dominates the asymptotic behavior for low values of frequency. It also relaxes the need to deal with some second-order and more complex nonlinear processes verified at low frequencies for a single interface. The second component is the circuit model, which describes best the polarization associated with the metal (or clay) electrolyte interface asymptotic behavior for medium to high frequencies. For this purpose three major contributions were analyzed (Chang and Jaffé, 1952; Grahame, 1952; Madden and Marshall, 1959a). I verified that the cases discussed by these authors, involving the possibility of transportation of electrical charge through induction and/or diffusion, chemical reactions (with or without ionic discharge, formation and accumulation of a product), chain reactions, and ionic recombination, can all be reduced for medium to high values of frequency to the lower branch in the circuit of Figure 1.

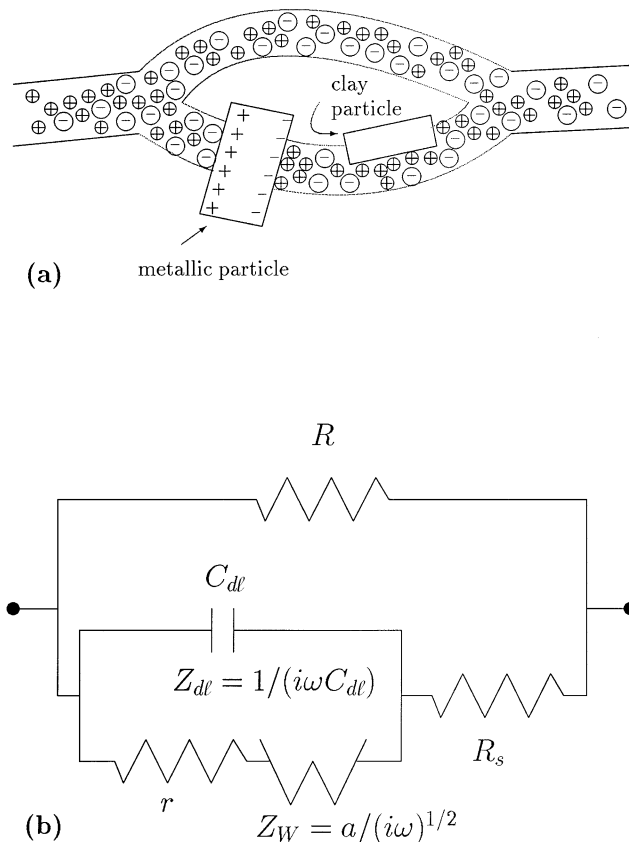


FIG. 1. (a) Schematic of low-frequency rock electrical polarization (IP). (b) The equivalent fundamental circuit analog as the unit cell for electrical polarization of rocks (Dias, 1968, 1972).

Such ideas have been used and/or referenced by several researchers (Morrison et al., 1969; Fuller and Wait, 1976; Cockburn and Goldman, 1982; Cockburn, 1985; Lima and Sharma, 1992). A thorough mathematical and numerical analysis of the basic function directed toward its use in applied problems is given by Cockburn (1983). However, the parameters of the original form of the conductivity function need rearranging to become better suited for manipulation in inversion problems and to the petrophysical interpretation of these parameters.

This paper has two objectives: (1) to present the constitutive function  $\sigma$  proposed by Dias (1968, 1972) in a new form that is more convenient to use in electromagnetic and petrophysical inversion problems involving polarizable rocks and (2) to demonstrate the potential of this function while providing a comparative analysis with other polarization models.

### CONSIDERATIONS ON A PARTICULAR MODEL

#### The old and the new conductivity functions

The original total current conductivity ( $\sigma$ ) given by Dias (1968, 1972), associated with the circuit analog of Figure 1, is reworked in terms of the new parameters defined in this section (Appendix B). This function was originally written in terms of five independent parameters with undefined limits of variation and unclear physical meanings. These reasons led me to redefine the parameters, keeping the same function. In its new form, the function is now derived directly from the circuit of Figure 1 as follows.

For such a purpose, let us first write the admittance function for the circuit of Figure 1 as

$$\frac{1}{Z} = \frac{1}{R} + \frac{1}{R_s + Z'}, \quad (1)$$

with

$$\frac{1}{Z'} = \frac{1}{Z_{C_{dl}}} + \frac{1}{r + Z_W}, \quad (2)$$

where  $Z_{C_{dl}}$  and  $Z_W$  represent, respectively, the impedance of the double-layer capacitance  $(i\omega C_{dl})^{-1}$  and the Warburg impedance  $a/(i\omega)^{1/2}$ , where  $i = \sqrt{-1}$  and  $a$  is a real constant. The value of  $1/Z$  for  $\omega = 0$  is  $1/R$ .

We then write for the conductivity,  $\sigma$ , normalized to its dc value,  $\sigma_0$ ,

$$\sigma/\sigma_0 = 1 + \frac{R}{R_s + \frac{(r+Z_W)Z_{C_{dl}}}{r+Z_W+Z_{C_{dl}}}} \quad (3)$$

or, after some algebra,

$$\sigma/\sigma_0 = 1 + \frac{R\lambda/Z_W}{1 + (r + R_s)\lambda'/Z_W}, \quad (4)$$

where

$$\lambda = 1 + \mu, \quad (5)$$

$$\lambda' = 1 + \left(1 - \frac{r}{r + R_s}\right)\mu, \quad (6)$$

and

$$\mu = \frac{r + Z_W}{Z_{C_{dl}}}. \quad (7)$$

#### The new parameters and function $\sigma$

Now let us represent function (4) using the following five parameters. For this, I define relaxation time, electrochemical parameter, pore length fraction, and chargeability keeping, however,  $\sigma_0$  as before.

Relaxation time is given by

$$\tau = rC_{dl}. \quad (8)$$

This parameter is positive and corresponds to the relaxation time of the electrical double-layer zone in the unit cell when diffusion is overwhelmed by the other mechanisms. It seems related to the average size of the particles producing polarization, as will be seen later.

Electrochemical parameter is given by

$$\eta = a/r. \quad (9)$$

This parameter has a physical dimension  $s^{-1/2}$  and is related to the relative significance between the ohmic (induced) electrical current component and the modulus of the diffusion-produced component inside the electrical double layer at 1 rad/s frequency in the unit cell. It is related to the characteristics of the electrochemical environment producing polarization. The corresponding parameter for a single metal-electrolyte interface is equal to  $2D^{1/2}/\ell$ , where  $D$  is the value of the cation diffusivity and  $\ell$  is the thickness of the electrical double layer (Chang and Jaffé, 1952). The value of  $\eta$  varies with cation concentration and the plate separation  $L$  in a solution (about 1 to 10 for  $L$  varying from 4 to 1 mm, according to Jaffé and Rider, 1952). Because  $\eta$  is dependent on  $\ell$ , it will not vary with frequency to a first approximation, as a consequence of linearization. Extending this definition to the rocks, the value of  $\eta$  could easily range from 1 or less to about 150. It is expected to increase with concentration, both of the disseminated sources of induced polarization (IP) and of the ions in solution, although less critically with the latter.

Pore length fraction affected by the source of polarization is given by

$$\delta = \frac{r}{r + R_s}. \quad (10)$$

This parameter is dimensionless and is defined on the interval  $0 \leq \delta < 1$ . It refers solely to the pore path that represents the locus where polarization is produced, and it involves only the components of the ohmic (induced) conduction. The parameter  $r$  is proportional to the length of the average zone affected by the presence of the electrical double layer and  $R_s$  to the extent not influenced by it in the same pore. So  $\delta$  is roughly the ratio of the size of the affected zone to the size of this same zone added to the size of the homogeneous solution zone next to it in the average unit cell.

Chargeability, according to Seigel (1959a,b) and Wait (1959b), is given by

$$m = \frac{\sigma_{\omega \rightarrow \infty} - \sigma_{\omega \rightarrow 0}}{\sigma_{\omega \rightarrow \infty}}. \quad (11)$$

This parameter, as  $\delta$ , is dimensionless and is defined in the interval  $0 \leq m < 1$ . It corresponds to the maximum dispersion in the amplitude of  $\sigma$  as a varying function of frequency, normalized to its maximum value (the value reached when this type of polarization is over) at the high frequencies. The saturation

frequencies are on the order of megahertz at the highest and  $10^{-3}$  Hz at the lowest (Dias, 1968, 1972).

When using the limit values obtained from equation (4), this parameter becomes

$$m = \frac{R}{R + R_s}. \quad (12)$$

Chargeability is the best defined and most reliable parameter used until now to identify rock polarization in field measurements. Its value is commonly associated with the intensity of the polarization effect.

Introducing the new parameters and performing some algebra, we rewrite equation (4) as

$$\sigma = \sigma_0 \left[ 1 + \alpha \frac{\lambda \beta (i\omega)^{1/2}}{1 + \lambda' \beta (i\omega)^{1/2}} \right], \quad (13)$$

where

$$\lambda = 1 + \mu, \quad (14)$$

$$\lambda' = 1 + (1 - \delta)\mu, \quad (15)$$

$$\mu = i\omega\tau[1 + \eta(i\omega)^{-1/2}], \quad (16)$$

$$\alpha = m(1 - \delta)/(1 - m), \quad (17)$$

and

$$\beta = (\eta\delta)^{-1}. \quad (18)$$

The function  $\sigma$  is now expressed in terms of one variable ( $\omega$ ) and five independent parameters ( $\sigma_0$ ,  $\tau$ ,  $\eta$ ,  $\delta$ , and  $m$ ).

In traditional exploration campaigns that use induced polarization, geophysicists have exploited only three parameters,  $\sigma_0$ ,  $\tau$ , and  $m$  [percent frequency effect (PFE) is a simplification of  $m$ ].

An expression for resistivity as the inverse of  $\sigma$ , after some algebra, is given by

$$\rho = \rho_0 \left[ 1 - m \left( 1 - \frac{1}{1 + i\omega\tau'(1 + \frac{1}{\mu})} \right) \right], \quad (19)$$

where  $\mu = i\omega\tau + (i\omega\tau'')^{1/2}$ , the same as in equations (7) and (16);  $\tau = rC_{de}$ ;  $\tau' = (R + R_s)C_{de}$ ;  $\tau'' = (aC_{de})^2$ ;  $m = (\rho_0 - \rho_\infty)/\rho_0$  (as before); and  $\rho_0$  is the real dc value of  $\rho$ . Note that  $\tau'/\tau = (1/\delta)(1 - \delta)/(1 - m)$  and  $\tau''/\tau^2 = \eta^2$ . Also note that the relaxation times ( $\tau$ ,  $\tau'$ , and  $\tau''$ ) appearing in equation (19) seem related to the different relaxation modes of the fundamental circuit.

### Particular cases deduced from the Dias model

For this purpose, consider equation (19). If  $\mu = i\omega\tau + (i\omega\tau'')^{1/2}$  has a modulus on the order of unity, then the complete function given by equation (19) must be maintained. If that is not so, two cases must be considered.

First, if  $|\mu| \gg 1$ , we can write straightforwardly

$$\rho = \rho_0 \left[ 1 - m \left( 1 - \frac{1}{1 + i\omega\tau'} \right) \right], \quad (20)$$

where  $\tau' = (R + R_s)C_{de}$ . Expression (20) corresponds to the classical Debye model. In terms of the fundamental circuit elements, this is equivalent to saying that  $|(r + Z_W)/Z_{Cde}| \gg 1$ . In terms of the conduction mechanisms, this indicates that

the double-layer capacitive effect conducts current more efficiently than the series combination of induction and diffusion mechanisms inside the double layer.

Second, if  $|\mu| \ll 1$ , we can approximate equation (19) by

$$\rho = \rho_0 \left[ 1 - m \left( 1 - \frac{1}{1 + \frac{i\omega\tau'}{i\omega\tau + (i\omega\tau'')^{1/2}}} \right) \right]; \quad (21)$$

that is,

$$\rho = \rho_0 \left[ 1 - m \left( 1 - \frac{1}{\frac{i\omega(\tau + \tau') + (i\omega\tau'')^{1/2}}{i\omega\tau + (i\omega\tau'')^{1/2}}} \right) \right]. \quad (22)$$

In terms of the equivalent fundamental circuit, this corresponds to  $|(r + Z_W)/Z_{Cde}| \ll 1$ . In terms of conduction mechanisms, it means that the capacitive effect is insignificant compared to the induction-diffusion series combined effect.

Two subcases can then be distinguished. First, when  $(\omega\tau'')^{1/2} \gg \omega\tau$ , the resulting resistivity is

$$\rho = \rho_0 \left[ 1 - m \left( 1 - \frac{1}{1 + (i\omega\tau_W)^{1/2}} \right) \right], \quad (23)$$

where  $\tau_W = (\tau + \tau')^2/\tau'' = [(r + R + R_s)/a]^2$ . Expression (23) corresponds to the so-called Warburg model (Pelton et al., 1978). In terms of the equivalent circuit, this corresponds to the situation where  $|Z_W/r| \gg 1$ . In terms of physical mechanisms, it means that the electrical current through the double layer is determined by a diffusion process.

In the second subcase when  $(\omega\tau'')^{1/2} \ll \omega\tau$ , the resulting resistivity is

$$\rho = \rho_0 \left[ 1 - m \left( 1 - \frac{1}{1 + \frac{\tau'}{\tau} \left( 1 - \frac{1}{(i\omega\tau^*)^{1/2}} \right)} \right) \right], \quad (24)$$

where  $\tau'/\tau = (R + R_s)/r$  and  $\tau^* = \tau^2/\tau'' = (r/a)^2$ . In terms of the equivalent circuit, this corresponds to  $|Z_W/r| \ll 1$ . In this case, induction dominates the current flowing through the double-layer zone. It corresponds to a peculiar situation in which the amplitude of  $\rho$  passes through an intermediate plateau distinct from the extremal asymptotic values while the phase passes through a depression. Such a peculiar frequency interval, when it exists, is given by

$$\eta^2 \ll \omega \ll 1/\tau. \quad (25)$$

It is important to note that this model has, as particular cases, three functions corresponding to Debye, Warburg, and real constant. Coincidentally, the same situation occurs with the Cole–Cole model (Pelton et al., 1978) by assigning the values 1, 1/2, and 0 to the parameter  $c$  in the exponent of  $(i\omega\tau)^c$  in the Cole–Cole function, where  $0 \leq c \leq 1$ . Intuitively, it seems reasonable to assume that all curves generated from Cole–Cole functions could be generated by the Dias model. Yet, since the Dias model is a five-parameter function and the Cole–Cole model is a four-parameter function, the opposite cannot be true.

### CONSIDERATIONS ON THE EXISTING MODELS

I now discuss the most common models that describe this effect. When a particular model does not bring an equivalent

circuit analog from its origin, I provide it and reduce them to a standard representation in terms of complex resistivity using, whenever possible, similar parameters. Table 1 summarizes the models.

Models 3 to 10 (see Table 1) can be described as a parallel combination of a pure resistor with a series combination of a resistor and an impedance  $Z'$ , the latter given as a frequency function (Figure 2, Table 2). In such cases, resistivity can be expressed by a single function, according to Appendix C, as

$$\rho = \rho_0 \left[ 1 - m \left( 1 - \frac{1}{1 + (R + R_1)/Z'} \right) (1 - Z'/Z'_0) \right], \quad (26)$$

where  $Z'_0$  is the dc value of  $Z'$ .

To keep expression (26) general, I assume that point  $\omega = 0$  is excluded from the dominion of variation of  $\omega$ , keeping the value for  $Z'$  at  $\omega = 0$ , given by  $Z'_0$ , as a fixed parameter in equation (26), as shown. This introduces no limitation in this representation and its practical use.

In the Debye model,  $Z' = 1/(i\omega C)$  and  $Z'/Z'_0 = 0$ :

$$\frac{R + R_1}{Z'} = [(R + R_1)C]i\omega = i\omega\tau, \quad (27)$$

where  $\tau = (R + R_1)C$ .

In the Madden and Cantwell model,  $Z' = a/(i\omega)^{1/4}$  and  $Z'/Z'_0 = 0$ :

$$\frac{R + R_1}{Z'} = \left( \frac{R + R_1}{a} \right) (i\omega)^{1/4} = (i\omega\tau)^{1/4}, \quad (28)$$

where  $\tau = [(R + R_1)/a]^4$ .

In the Warburg model,  $Z' = a/(i\omega)^{1/2}$  and  $Z'/Z'_0 = 0$ :

$$\frac{R + R_1}{Z'} = \left( \frac{R + R_1}{a} \right) (i\omega)^{1/2} = (i\omega\tau)^{1/2}, \quad (29)$$

where  $\tau = [(R + R_1)/a]^2$ .

In the Cole–Cole model,  $Z' = a/(i\omega)^c$  and  $Z'/Z'_0 = 0$ :

$$\frac{R + R_1}{Z'} = \left( \frac{R + R_1}{a} \right) (i\omega)^c = (i\omega\tau)^c, \quad (30)$$

where  $\tau = [(R + R_1)/a]^{1/c}$ .

In the Zonge model,  $Z' = (R + R_1)/(\theta \mathcal{L}(\theta))$ , where  $\mathcal{L}(\theta) = \coth \theta - (1/\theta)$  is the Langevin function and  $Z'/Z'_0 = 0$ :

$$\frac{R + R_1}{Z'} = \theta \mathcal{L}(\theta), \quad (31)$$

where  $\theta = (i\omega\tau)^{c/2}$ ,  $\tau = [(R + R_1)/a]^{1/c}$  and  $0 \leq c \leq 1$ , the parameter  $a$  having the physical meaning shown in the corresponding circuits in Table 1.

Envelope functions for the Zonge model are determined by its asymptotic forms. When  $|\theta| \ll 1$ , the function  $\mathcal{L}(\theta)$  approaches  $\theta/3$  and equation (31) becomes a Cole–Cole-type function of exponent  $c$  and relaxation time  $\tau/3^{1/c}$ . When  $|\theta| \gg 1$ ,  $\mathcal{L}(\theta)$  approaches 1 and equation (31) becomes another Cole–Cole function with exponent  $c/2$  and relaxation time  $\tau$ . When plotted on an Argand plane, Zonge model curves are reduced to a Cole–Cole arc of a circle of smaller radius, for the smaller values of frequency, and depart toward another Cole–Cole arc of greater radius for the higher values of  $\omega$ . Both asymptotic arcs start and finish at the same points on the real axis, given by  $\rho_0$  at  $\omega = 0$  and  $(1 - m)\rho_0$  at  $\omega = \infty$ . The original Zonge model (Zonge, 1972) specified  $c = 1/2$ , having

then as asymptotes Warburg and Madden & Cantwell-type curves. The modification leading to Cole–Cole general function asymptotes was introduced by Pelton (1977).

The dual representation of the Zonge model (see Table 1) either through a network circuit system or an equivalent fundamental circuit conveniently shows the reasoning behind these two procedures for generating the same function representation to describe rock polarization.

In the Dias model,  $Z' = [r + a/(i\omega)^{1/2}]/[1 + (r + a/(i\omega)^{1/2}) \times i\omega C_{dl}]$  and  $Z'/Z'_0 = 0$ :

$$\begin{aligned} \frac{R + R_1}{Z'} &= i\omega(R + R_1)C_{dl} \left[ 1 + \frac{1}{i\omega r C_{dl} + (i\omega)^{1/2} a C_{dl}} \right] \\ &= i\omega\tau' \left[ 1 + \frac{1}{i\omega\tau + (i\omega\tau')^{1/2}} \right], \end{aligned} \quad (32)$$

where  $\tau = rC_{dl}$ ,  $\tau' = (R + R_1)C_{dl}$ , and  $\tau'' = (aC_{dl})^2$ .

In the Davidson–Cole model,  $Z' = (a/\omega_L^c)/(1 + i\omega/\omega_L)^c$  and

$$\frac{Z'}{Z'_0} = \frac{1}{(1 + i\omega\tau)^c}, \quad (33)$$

where  $\tau = 1/\omega_L$ . As a constraint relation, it is assumed that  $(R + R_1)/Z'_0 \gg 1$ .

In the generalized Cole–Cole model,  $Z' = (a/\omega_L^{ck})/[1 + (i\omega/\omega_L)^c]^k$  and

$$\frac{Z'}{Z'_0} = \frac{1}{[1 + (i\omega\tau)^c]^k}, \quad (34)$$

where  $\tau = 1/\omega_L$ . The same constraint relation is assumed as in the previous case.

Model 11 in Table 1, referred to as the multi-Cole–Cole model, can be described, as shown in Figure 3, as a parallel combination of two Cole–Cole circuits if at least one of the following conditions is satisfied (see Appendix C): (1)  $R_1 \gg R' \gg R''$ , (2)  $R_2 \gg R'' \gg R'$ , or (3)  $R_1 \gg R'$  and  $R_2 \gg R''$ . The resulting complex resistivity is

$$\begin{aligned} \rho &= \rho_0 \left[ 1 - m_1 \left( 1 - \frac{1}{1 + (i\omega\tau_1)^{c_1}} \right) \right] \\ &\times \left[ 1 - m_2 \left( 1 - \frac{1}{1 + (i\omega\tau_2)^{c_2}} \right) \right]. \end{aligned} \quad (35)$$

From the individual Cole–Cole circuits that make up Figure 3, one can obtain the expressions for  $\tau_1$ ,  $m_1$ ,  $\tau_2$ , and  $m_2$  and write

$$\tau_1/\tau_2 = \frac{[R'/(m_1 a_1)]^{1/c_1}}{[R''/(m_2 a_2)]^{1/c_2}}. \quad (36)$$

In practical cases, it is common that  $c_1 \simeq c_2$  and then

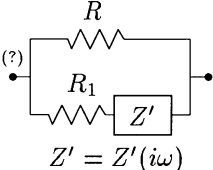
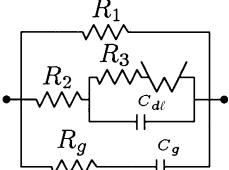
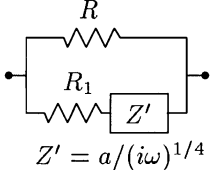
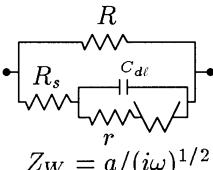
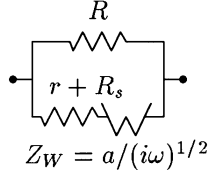
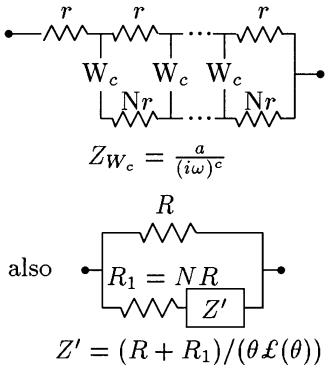
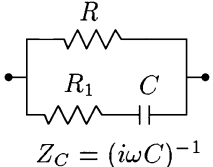
$$\tau_1/\tau_2 \simeq \left( \frac{R'/(m_1 a_1)}{R''/(m_2 a_2)} \right)^{1/c}, \quad (37)$$

where  $c$  is the average value of  $c_1$  and  $c_2$ .

It is also very common in practical cases that  $\tau_1$  and  $\tau_2$  are of very different orders of magnitude and that most of this contrast does not result from the  $m_1/m_2$  ratio. So one can write approximately

$$\tau_1/\tau_2 \simeq \left( \frac{R'/a_1}{R''/a_2} \right)^{1/c}. \quad (38)$$

**Table 1. Chronological listing of existing models with references, equivalent circuit analogs, and associated complex resistivities.**

Item	Model/reference	Circuit	Complex resistivity
1	Wait (1959a)	 $Z' = Z'(i\omega)$	$\rho = \rho_s \left( 1 - \frac{A}{1+2A/3} \right)$ <p><math>A</math> = average polarizability per unit volume of an infinite heterogeneous medium  <math>\rho_s</math> = resistivity of the host medium</p>
2	Ward and Fraser (1967)	 $Z_W = a/(i\omega)^{1/2}$	$\rho = \rho_D \left[ 1 - \frac{1}{1+(\rho_g + \gamma/i\omega)/\rho_D} \right]$ <p><math>\rho_D</math> = resistivity function associated with Dias model</p>
3	Madden and Cantwell (1967)	 $Z' = a/(i\omega)^{1/4}$	$\rho = \rho_0 \left[ 1 - m \left( 1 - \frac{1}{1+(i\omega\tau)^{1/4}} \right) \right]$ $m = (\rho_0 - \rho_\infty)/\rho_0 = \frac{R}{R+R_1}$ $\tau = ((R + R_1)/a)^4$
4	Dias (1968, 1972)	 $Z_W = a/(i\omega)^{1/2}$	$\rho = \rho_0 \left[ 1 - m \left( 1 - \frac{1}{1+i\omega\tau'(1+\mu^{-1})} \right) \right]$ $m = (\rho_0 - \rho_\infty)/\rho_0 = \frac{R}{R+R_s}$ $\mu = i\omega\tau + (i\omega\tau'')^{1/2}$ $\tau = rC_{dl}; \quad \tau' = (R + R_s)C_{dl}$ $\tau'' = (aC_{dl})^2$
5	Warburg Dias (1968, 1972) Pelton (1977)	 $Z_W = a/(i\omega)^{1/2}$	$\rho = \rho_0 \left[ 1 - m \left( 1 - \frac{1}{1+(i\omega\tau)^{1/2}} \right) \right]$ $m = (\rho_0 - \rho_\infty)/\rho_0 = \frac{R}{(r+R_s)+R}$ $\tau = \left( \frac{r+R_s+R}{a} \right)^2$
6	Zonge (1972) Pelton (1977)	 $Z_{W_c} = \frac{a}{(i\omega)^c}$ <p>also</p> $Z' = (R + R_1)/(\theta \mathcal{L}(\theta))$	$\rho = \rho_0 \left[ 1 - m \left( 1 - \frac{1}{1+\theta \mathcal{L}(\theta)} \right) \right]$ $\theta = (i\omega\tau)^{c/2}$ $\mathcal{L}(\theta) = \coth \theta - \frac{1}{\theta}$ $m = (\rho_0 - \rho_\infty)/\rho_0 = \frac{R}{R+R_1}$ $\tau = \left( \frac{R+R_1}{a} \right)^{1/c}; \quad 0 \leq c \leq 1$ $0 < N \leq 1$
7	Debye Pelton (1977)	 $Z_C = (i\omega C)^{-1}$	$\rho = \rho_0 \left[ 1 - m \left( 1 - \frac{1}{1+i\omega\tau} \right) \right]$ $m = (\rho_0 - \rho_\infty)/\rho_0 = \frac{R}{R+R_1}$ $\tau = C(R + R_1)$

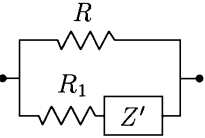
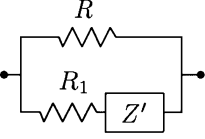
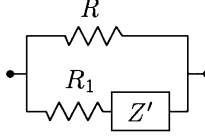
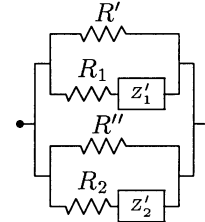
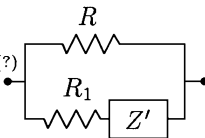
Expression (38) shows that if  $\tau_1$  and  $\tau_2$  exhibit different orders of magnitude, the material system must correspond necessarily to a petrophysical/electrochemical system with two distinct phases for such time constants to be physically meaningful.

Looking at it another way, let us consider which physical implications arise from the constraints set on the circuit components of Figure 3. Conditions 1 ( $R_1 \gg R' \gg R''$ ) and 2 ( $R_2 \gg R'' \gg R'$ ) suggest that pore constriction is somewhat

present either in one or the other of the two phases, right at the branch of the Cole–Cole individual circuits where polarization is produced. Condition 3 ( $R_1 \gg R'$  and  $R_2 \gg R''$ ) suggests the existence of pore constriction in each branch of the individual circuits where the sources of polarization are set on both phases of the system.

Conditions 1 and 2 reinforce the point that the multi-Cole–Cole model is tied to a multiphase physical system in terms of the polarization setting. Condition 3 could be compatible

**Table 1. (Continued.)**

Item	Model/reference	Circuit	Complex resistivity
8	Cole–Cole Pelton (1977)	 $Z' = a/(i\omega)^c$	$\rho = \rho_0 \left[ 1 - m \left( 1 - \frac{1}{1+(i\omega\tau)^c} \right) \right]$ $m = \frac{R}{R+R_1}; 0 \leq c \leq 1$ $\tau = \left( \frac{R+R_1}{a} \right)^{1/c}$
9	Davidson–Cole Pelton (1977)	 $Z' = a/(\omega_L + i\omega)^c$ <p>with <math>(R + R_1)/(a/\omega_L^c) \gg 1</math></p>	$\rho = \rho_0 \left[ 1 - m \left( 1 - \frac{1}{(1+i\omega\tau)^c} \right) \right]$ $m = \frac{R}{R+R_1} \frac{a/\omega_L^c}{R_1 + a/\omega_L^c}; 0 \leq c \leq 1$ $\tau = 1/\omega_L$
10	Generalized Cole–Cole Pelton (1977)	 $Z' = a/(\omega_L^c + (i\omega)^c)^k$ <p>with <math>(R + R_1)/(a/\omega_L^{ck}) \gg 1</math></p>	$\rho = \rho_0 \left[ 1 - m \left( 1 - \frac{1}{[1+(i\omega\tau)^c]^k} \right) \right]$ $m = \frac{R}{R+R_1} \frac{a/\omega_L^{ck}}{R_1 + a/\omega_L^{ck}}$ $0 \leq (c; k) \leq 1$ $\tau = 1/\omega_L$
11	Multi-Cole–Cole Pelton et al. (1978)	 $Z'_j = a_j/(i\omega)^{c_j}; j=1,2$ <p>at least one of the following conditions satisfied:</p> <ol style="list-style-type: none"> <li>1) <math>R_1 \gg R' \gg R''</math></li> <li>2) <math>R_2 \gg R'' \gg R'</math></li> <li>3) <math>R_1 \gg R'; R_2 \gg R''</math></li> </ol>	$\rho = \rho_0 \left[ 1 - m_1 \left( 1 - \frac{1}{1+(i\omega\tau_1)^{c_1}} \right) \right]$ $\cdot \left[ 1 - m_2 \left( 1 - \frac{1}{1+(i\omega\tau_2)^{c_2}} \right) \right]$ $m_1 = \frac{R'}{R_1+R'}; 0 \leq (c_1; c_2) \leq 1$ $\tau_1 = \left( \frac{R_1+R'}{a_1} \right)^{1/c_1}$ $m_2 = \frac{R''}{R_2+R''}$ $\tau_2 = \left( \frac{R_2+R''}{a_2} \right)^{1/c_2}$
12	Wong (1979)	 $Z' = Z'(\omega)$	$\rho = \rho_s \left( 1 - \frac{3 \sum_j N_j f_j}{1 + 2 \sum_j N_j f_j} \right)$ <p><math>N_j</math> = number of spherical particles <math>j</math> per unit volume  <math>f_j</math> = reflection coefficient at the interface between a homogeneous infinite ionic solution and the medium <math>j</math>  <math>\rho_s</math> = resistivity of the homogeneous solution</p>

with a single-phase system if the ratio  $\tau_1/\tau_2$  would not be very different from 1.

The Wait (1959a) and Wong (1979) models (Table 1) are constructed on a similar physical structure. They consist of small spherical metallic particles, regularly spaced (Wait) or randomly spaced (Wong), distributed in a continuum and separated from each other by distances far enough to avoid mutual electric interference among the induced dipoles. In Wait's model, each particle is covered by a dielectric film to simulate the interfacial electrical mechanism and to ensure a perfectly polarizable sphere using a strictly macroscopic approach. In Wong's model, electrochemical principles are used to obtain more realistic reflection coefficients at the interfaces. In both models, the reflection coefficients are introduced into the expression derived by Maxwell (1891) for the complex resistivity of a heterogeneous mixture. An equivalent circuit analog for such cases is hard to portray, except in a rather simple way, as shown in Table 1.

Model 2 in Table 1 is suggested by Ward and Fraser (1967). It was very helpful for the initial insight into the Dias model.

The Drake model described in Van Voorhis et al. (1973) and a model used by Nelson et al. (1982) generate functions reducible, respectively, to the Davidson–Cole model (when the coefficient  $m$  is close to 1) and to the Warburg or Cole–Cole models. For that reason, these models are not discussed further.

#### MODELS' COMPARATIVE PERFORMANCE

Each model owes its origin to the fact that, to a greater or lesser extent and precision, it was verified that the model was

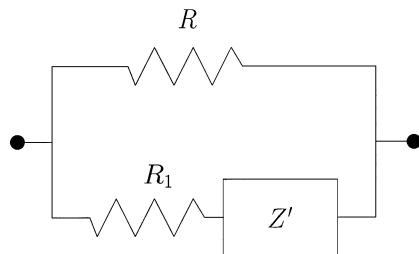


FIG. 2. Schematic equivalent fundamental circuit analog for many IP models shown in Table 2. The value  $Z'$  is a characteristic frequency function.

good to describe some reliable experimental data. I do not intend to survey all cases in which a given model is good; instead, I select a few representative data samples that, by their peculiar complexity, can be used to test the capacity of the various models to fit them.

Consider three samples of data. The first is the case consisting of phase spectrum experimental data in the frequency range  $10^{-2}$  to  $10^3$  Hz, originally studied by Nelson et al. (1982) and shown in Figure 4. This case shows that more general models, such as the multi-Cole–Cole and Dias models, can describe the same experimental data even better than the original (Warburg) model (see Figure 4). In the order cited, the percent rms errors for each model are, respectively, 4.6%, 7.8%, and 12.8%.

According to Nelson et al. (1982), these data relate to the core sample NW-1-584 in a drill hole sequence consisting of a spotted siltstone, very fine-grained dark gray rock composed of 25–30% quartz, 30–35% plagioclase, 5–7% muscovite, 7–10% chlorite, 7–10% graphite, and 5–7% pyrite. The pyrite is 0.01–1.0 mm, disseminated and vein; the veins occur in the most pyrite-rich parts of the bed. Pyrite concentration varies from

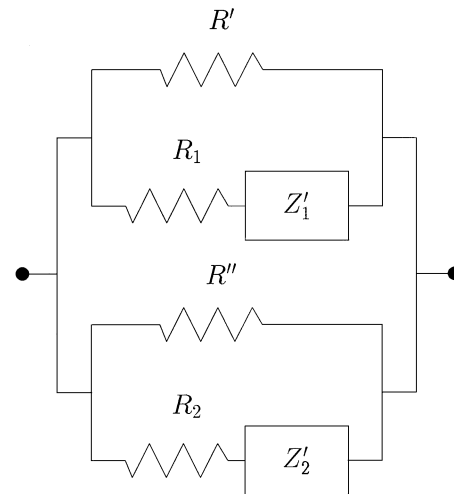


FIG. 3. Schematic equivalent fundamental circuit analog for the multi-Cole–Cole model, where  $Z'_j = a_j/(i\omega)^{c_j}$  and  $j = 1, 2$ , assuming at least one of the following conditions is satisfied: (1)  $R_1 \gg R' \gg R''$ ; (2)  $R_2 \gg R'' \gg R'$ ; (3)  $R_1 \gg R'$  and  $R_2 \gg R''$ .

**Table 2. Family of models having Figure 2 for a circuit analog with the associated function  $Z'$  and impedances at frequencies 0 and  $\infty$ . Chargeability,  $m$ , is defined as  $(Z_0 - Z_\infty)/Z_0$ .**

Item	model	$Z'$	$Z_0$	$Z_\infty$	$m$
1	Debye	$C^{-1}/(i\omega)$	$R$	$RR_1/(R + R_1)$	$R/(R + R_1)$
2	Madden and Cantwell	$a/(i\omega)^{1/4}$	$R$	$RR_1/(R + R_1)$	$R/(R + R_1)$
3	Warburg	$a/(i\omega)^{1/2}$	$R$	$RR_1/(R + R_1)$	$R/(R + R_1)$
4	Cole–Cole	$a/(i\omega)^c$	$R$	$RR_1/(R + R_1)$	$R/(R + R_1)$
5	Zonge*	$(R + R_1)/(\theta \mathcal{E}(\theta))$	$R$	$RR_1/(R + R_1)$	$R/(R + R_1)$
6	Dias	$\frac{r+a/(i\omega)^{1/2}}{1+i\omega C_d \mathcal{E}[r+a/(i\omega)^{1/2}]}$	$R$	$RR_1/(R + R_1)$	$R/(R + R_1)$
7	Davidson–Cole†	$\frac{a}{(\omega_L + i\omega)^c}$	$\frac{R}{1 + \frac{R}{R_1 + Z_0}}$	$RR_1/(R + R_1)$	$\frac{R/(R + R_1)}{1 + R_1/Z_0}$
8	Generalized Cole–Cole†	$\frac{a}{[\omega_L^c + (i\omega)^c]^k}$	$\frac{R}{1 + \frac{R}{R_1 + Z_0}}$	$RR_1/(R + R_1)$	$\frac{R/(R + R_1)}{1 + R_1/Z_0}$

\*Function  $\mathcal{E}(\theta) = \coth \theta - (1/\theta)$ , where  $\theta = (i\omega\tau)^{c/2}$ .

†Using  $(R + R_1)/Z_0 \gg 1$  as a constraint.



<1% to 20% from top to bottom (or bottom to top) of beds 1 to 2 cm thick.

The second sample is the case consisting of amplitude and phase spectra experimental data in the frequency range  $10^{-3}$  to  $10^3$  Hz, originally studied by Klein and Sill (1982) and shown in Figure 5. This case shows the failure of the generalized Cole–Cole model to describe the phase data in the section of the spectrum from about 30 Hz to  $10^3$  Hz. One must remember that the generalized Cole–Cole model includes Cole–Cole and Davidson–Cole models as particular cases. Figure 5 also shows that, with this data, both amplitude and phase can be totally described by multi-Cole–Cole and Dias models, with percent

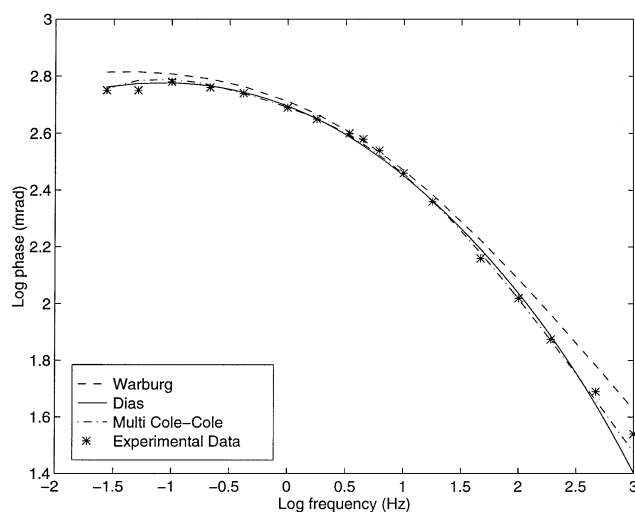


FIG. 4. Phase measurements and Warburg model fitting by Nelson et al. (1982) for a core sample containing disseminated metallics. Multi-Cole–Cole and Dias models best fitting of data is done by the author. Coefficients for each model are listed in row 1 of Table 3.

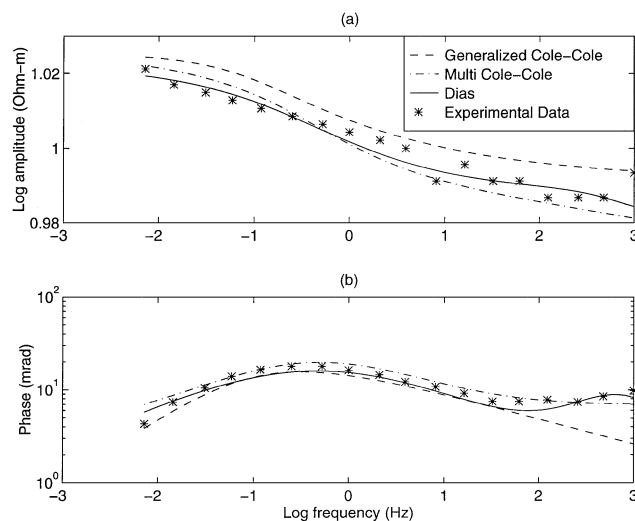


FIG. 5. Generalized Cole–Cole model best fitting of experimental data for a synthetic sample consisting of a mixture of 3% by weight Ca-montmorillonite plus glass beads of  $4.0\text{--}12.5 \times 10^{-5}$  m diameter (Klein and Sill, 1982). Multi-Cole–Cole and Dias models best fitting of data is done by the author. Coefficients of each model are listed in row 2 of Table 3. Spectrum for amplitude is shown in (a), for phase in (b).

rms errors (amplitude and phase) given, respectively, by (1.0%, 20%) and (0.68%, 14%).

According to Klein and Sill (1982), these data relate to a synthetic mixture of 3% dry weight Ca-montmorillonite (84.4 meq/100 g), plus fine-grain-size glass beads (0.040–0.125 mm diameter) saturated with  $10^{-2}$  molar NaCl electrolyte.

The third sample is the case consisting of amplitude and phase spectra experimental data in the frequency range  $10^{-2}$  to  $10^6$  Hz, originally studied by Mahan et al. (1986) and shown in Figures 6 and 7. This case shows the failure of Debye, Warburg, and Wong models in describing both amplitude and phase in the portion of the spectrum above  $10^3$  Hz (see Figure 6). It is well known that simple Cole–Cole functions possess only one maximum for phase and amplitude; this is also true for Zonge

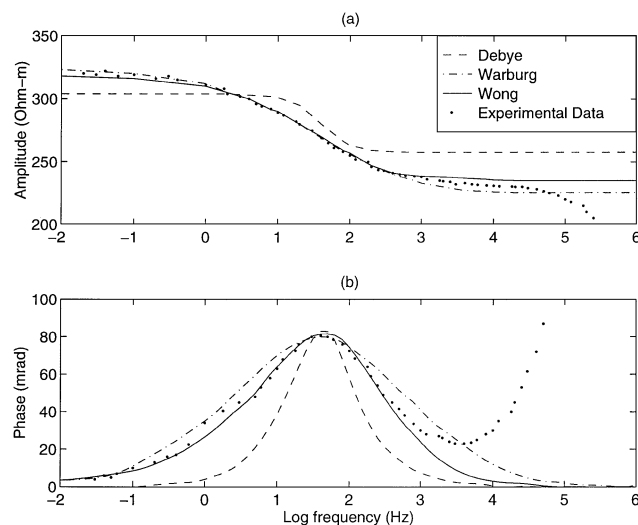


FIG. 6. Wong, Warburg, and Debye models best fitting of experimental data for a synthetic sample consisting of a mixture of 6.5% chalcopryite of 150–125  $\mu\text{m}$  radii, disseminated in a matrix of quartz sand of grain size  $<53 \mu\text{m}$  saturated with NaCl  $10^{-3}$  M electrolyte (Mahan et al., 1986). Spectrum for amplitude is shown in (a), for phase in (b).

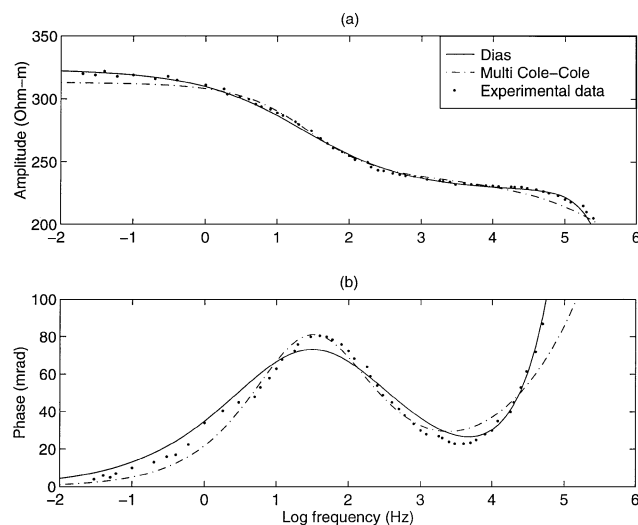


FIG. 7. Same experimental data of Figure 6. Best fitting is done by the author for multi-Cole–Cole and Dias models. Coefficients for each model are listed in row 3 of Table 3. Spectrum for amplitude is shown in (a), for phase in (b).

model curves, since each of these curves is bounded asymptotically by two Cole–Cole curves. Consequently, the Zonge model is unable to describe the experimental data of Figure 6. Instead, Figure 7 shows the same data being properly described for both amplitude and phase in the whole spectrum by multi-Cole–Cole and Dias models, with percent rms errors (amplitude and phase) given, respectively, by (1.4%, 22%) and (0.8%, 24%).

According to Mahan et al. (1986), these data relate to a synthetic sample with the following characteristics: 6.5% vol. chalcopryrite of 0.150–0.125 mm grain radii, disseminated in a matrix consisting of quartz sand, grain size  $<53 \mu\text{m}$  (without any cementing agent), 34.3% porosity, saturated with a  $10^{-3}$  molar NaCl electrolyte. This mixture was held in place within a plastic tube whose end faces were covered with filter paper.

The experimental data fitting provided the coefficients shown in Table 3.

### COEFFICIENTS: PETROPHYSICAL INTERPRETATION

The purpose of this section is to show how reasonable the values of the coefficients are when generated by our model and to clarify their associated petrophysical meanings.

The agreement in the values of  $\rho_0$  is evident among the various models tested for the cases analyzed (Table 3). The same applies to the magnitude of  $m$  (if one takes for the multi-Cole–Cole model only that value closer to the ones given by the other models).

Concerning the petrophysical information provided by these coefficients, the core samples analyzed by Nelson et al. (1982) and Mahan et al. (1986) are expected to correspond to strong magnitudes of the dispersion effect, as actually shown by the large values of  $m$  obtained from the models. The same kind of agreement exists concerning the small values of  $m$  obtained from the models for the core sample analyzed by Klein and Sill (1982).

Quite different values of  $\tau$  were generated by the various models. The best possible way to check their validity is to look for the average particle sizes which these values of  $\tau$  correspond to in the curve constructed by Olhoeft (1985) and to compare them with experimental information. Table 4 shows that Dias' model exhibits a far better agreement with the experimental data than the other models in that table.

Parameters  $\eta$  and  $\delta$  pertain just to our model. The first is supposed to have a strong dependence on the separation between

**Table 3. Coefficients entered in the models to describe experimental data.**

Model	Coefficients				
Warburg*		$m = 0.990$	$\tau = 398 \text{ s}$		
Multi-CC*		$m_1 = 0.832$	$\tau_1 = 15.0 \text{ s}$	$c_1 = 0.671$	
		$m_2 = 0.754$	$\tau_2 = 0.345 \text{ s}$	$c_2 = 0.575$	
Dias*		$m = 0.977$	$\tau = 1.86 \times 10^{-4} \text{ s}$	$\delta = 0.037$	$\eta = 119 \text{ s}^{-1/2}$
Gener. CC†	$\rho_0 = 10.6 \text{ ohm-m}$	$m = 0.075$	$\tau = 1.8 \text{ s}$	$c = 0.72$	$k = 0.38$
Multi-CC†	$\rho_0 = 10.8 \text{ ohm-m}$	$m_1 = 0.059$	$\tau_1 = 0.368 \text{ s}$	$c_1 = 0.6$	
		$m_2 = 0.18$	$\tau_2 = 1.0 \times 10^{-7} \text{ s}$	$c_2 = 0.1$	
Dias‡	$\sigma_0^{-1} = 10.5 \text{ ohm-m}$	$m = 0.089$	$\tau = 2.41 \times 10^{-4} \text{ s}$	$\delta = 0.181$	$\eta = 9.7 \text{ s}^{-1/2}$
Multi-CC‡	$\rho_0 = 313 \text{ ohm-m}$	$m_1 = 0.988$	$\tau_1 = 2.3 \times 10^{-8} \text{ s}$	$c_1 = 0.452$	
		$m_2 = 0.238$	$\tau_2 = 6.24 \times 10^{-3} \text{ s}$	$c_2 = 0.670$	
Dias§	$\sigma_0^{-1} = 323 \text{ ohm-m}$	$m = 0.786$	$\tau = 1.02 \times 10^{-6} \text{ s}$	$\delta = 0.884$	$\eta = 19 \text{ s}^{-1/2}$

\*Experimental data: Nelson et al., 1982.

†Experimental data: Klein and Sill, 1982.

‡Experimental data: Mahan et al., 1986.

**Table 4. Particle size determined from the values of  $\tau$ , by using the curve of time constant versus radius of particle (Olhoeft, 1985).**

Model	$\tau \text{ (s)}$	Particle size	
		Interpreted (mm)	Experimental (mm)
Dias	$1.9 \times 10^{-4}$	$5 \times 10^{-2}$	$10^{-2}-1$ (5–7% py)†
Multi-CC	$\tau_1 = 15$	35	size? (7–10% graph)†
	$\tau_2 = 0.35$	2	
Warburg	$4 \times 10^2$	$>10^2$	
Dias	$2.4 \times 10^{-4}$	$6 \times 10^{-2}$	$10^{-2}-0.3^*$ (3% clay particles)‡
Multi-CC	$\tau_1 = 3.7 \times 10^{-1}$	2	$4 \times 10^{-2}-0.125$ (glass beads)‡
	$\tau_2 = 1.0 \times 10^{-7}$	$0.8 \times 10^{-3} - 10^{-2}$	
Gener. CC	1.8	9	
Dias	$1.0 \times 10^{-6}$	$0.4 \times 10^{-2**}$	$0.125 - 0.150$ (6.5% cpy)§
Multi-CC	$\tau_1 = 2.3 \times 10^{-8}$	$3 \times 10^{-4}$	$<0.53 \times 10^{-1}$ (qtz sand)§
	$\tau_2 = 6.2 \times 10^{-3}$	0.7	

\*Estimated size.

\*\*Uncertain; no experimental information supporting.

py = pyrite; cpy = chalcopryrite; graph = graphite; qtz = quartz.

†Source: Nelson et al., 1982.

‡Source: Klein and Sill, 1982.

§Source: Mahan et al., 1986.

**Table 5. Relationship between the values of  $\eta$  and the volume concentration of IP sources.**

$\eta$ ( $s^{-1/2}$ )	Experimental data
119	5–7% py, 7–10% graph, conc.= (?) <sup>*</sup>
19	6.5% cpy, conc.= $10^{-3}$ M NaCl <sup>†</sup>
9.7	3% Ca-montmorillonite, conc.= $10^{-2}$ M NaCl <sup>‡</sup>

py = pyrite; cpy = chalcopyrite; graph = graphite.

<sup>\*</sup>Source: Nelson et al., 1982.

<sup>†</sup>Source: Mahan et al., 1986.

<sup>‡</sup>Source: Klein and Sill, 1982.

particles (sources of IP) and a weak dependence (something like 1/4 power) on the ionic concentration in solution. Since  $\eta$  must increase to the limit when the volume distribution of the particles gets tight, it is supposed to increase within certain limits with the number of particles per unit volume. This is verified from Table 5.

As to the petrophysical property associated with  $\delta$ , namely, the ratio of the size of the affected zone (nearly the thickness of the double layer) to the size of this same zone added to the homogeneous zone next to it, there is no experimental information in the data analyzed for a true comparison. Nonetheless, the sample of Klein and Sill (1982) permits one to compute the value for a coefficient  $A = (1 - \delta)/\delta$  using the value of  $\delta$  given by our model and obtaining  $A = 4.52$ , which is in the range ascribed by these authors to  $A$  (0.1 to 10).

### DISCUSSION

Based on the selected cases presented here, two models out of those analyzed to describe IP can survive confronting the experimental data shown: the multi-Cole–Cole and Dias models. This is also supported in a more extensive survey being conducted by the author.

When comparing models, two aspects must be kept in mind. The first is the nonuniqueness (ambiguity) in the determination of the coefficients of the main function when inverted, searching for the petrophysical inherent informations possibly existing in them. This ambiguity increases with the number of coefficients. In this sense, when two models equally describe the same experimental data, the one having the smaller number of coefficients is expected to be less ambiguous if not unique. The second is the existence or not of a physical meaning interpretable from such coefficients. This aspect favors a model constructed on a phenomenological reasoning and possessing coefficients with petrophysical meaning defined from origin, when compared to another built empirically. In this respect, the multi-Cole–Cole model, although good to superimpose experimental data, often has an unclear and inconsistent physical meaning interpretable through its coefficients. This is clearly shown, for instance, by the single-phase electrochemical medium described in Figure 7 as a double Cole–Cole model.

Despite the small number of cases analyzed, for the very diverse cases considered here the Dias model yields excellent consistency.

### CONCLUSIONS

The model set by Dias (1968, 1972) has much to offer, and its potential has not yet been fully explored to describe petrophysical properties of rocks through measurements of electrical polarization.

In its new reparameterized form presented here, the new total current conductivity function uses parameters that have from their origin petrophysical meaning and well-defined intervals of variation. The function itself now has more appeal for inverse problems, both for electromagnetic and petrophysical purposes.

In the broad context in which this model is presented, an analysis was made, with some classical models being derived as particular cases. A generating function was also introduced, from which most of the existing models (all the models representable by the equivalent fundamental circuit analog in Figure 2) can be derived. Also, new equivalent circuit analogs were written for Zonge, Davidson–Cole, generalized Cole–Cole, and multi-Cole–Cole models. In the latter case, the introduced equivalent circuit imposed intrinsic constraints on the relative values of the circuit elements to generate the associated final function. The constraint relations combined with the analysis of the relaxation times ratio suggest that, for such a model to be justified, a physical association must exist connecting a multistage Cole–Cole function to a multiphase electrochemical/petrophysical system. This point establishes a physical criterion to check the validity of this model.

The experimental data displayed, while limited to a few specially selected cases, permitted a comparison of performance and discussion of the various existing models and discussed the consistency of the petrophysical meaning associated with their coefficients. These results suggest that only the multi-Cole–Cole and Dias models have adequate structure to cope with the most intricate experimental data curves. Since the multi-Cole–Cole model is expressed through a function of seven coefficients and the Dias model by a function of five, the latter has less ambiguity in coefficient determination. Also, since the first model is empirical while the second is phenomenological, it seems reasonable that a full analysis of cases using the Dias model is worthwhile to check (a) its capacity to describe all the reliable experimental data available and (b) the petrophysical meaning of its coefficients and the corresponding interpretation consistency.

### ACKNOWLEDGMENTS

This paper has benefitted from the encouragement of S. Treitel and reviews by James R. Wait, Phillip H. Nelson, William Frangos, Gary R. Olhoeft, and David L. Alumbaugh. Their critical comments and suggestions are greatly appreciated. I also thank Olivar A. L. Lima and Allen Q. Howard, Jr., for carefully reading the manuscript and Licurgo P. Brito and Emerson R. Rodrigues for assistance during the typesetting. This research is supported by the Brazilian National Council for Scientific and Technological Development (CNPq) and the Laboratory for Petroleum Engineering and Exploration at North Fluminense State University.

### REFERENCES

- Angoran, Y., and Madden, T. R., 1977, Induced polarization—A preliminary study of its chemical basis: *Geophysics*, **42**, 788–803.
- Bockris, J. O., and Reddy, A. K. N., 1970, *Modern electrochemistry*: Plenum Press.
- Brant, A. A., 1959, Historical summary of overvoltage developments by Newmont Exploration Limited 1946–1955, in Wait, J. R., Ed., *Overvoltage research and geophysical applications*: Pergamon Press, Internat. Series on Earth Sciences, **4**, 1–3.

- Chang, H. C., and Jaffé, G., 1952, Polarization in electrolytic solutions, part I: Theory: *J. Chem. Phys.*, **20**, 1071–1077.
- Cockburn, B., 1983, Étude mathématique et numérique des equation de Maxwell dans des milieux polarisable: Ph.D. thesis, Univ. Paris IX.
- 1985, Numerical resolution of Maxwell's equations in polarizable media at radio and lower frequencies: *J. Sci. Stat. Comput.*, **6**, 843–852.
- Cockburn, B., and Goldman, Y., 1982, Modèle Maxwell-Dias (1D) dans un milieu polarisable: Comparaison de deux méthodes de résolution numérique: 15<sup>ème</sup> Colloque d'Analyse Numérique.
- Collet, L. S., and Katsube, T. J., 1973, Electrical parameters of rocks in developing geophysical techniques: *Geophysics*, **38**, 76–91.
- Dias, C. A., 1968, A non-grounded method for measuring electrical induced polarization and conductivity: Ph.D. thesis, Univ. California–Berkeley.
- 1972, Analytical model for a polarizable medium at radio and lower frequencies: *J. Geophys. Res.*, **77**, 4945–4956.
- Evjen, H. M., 1948, Theory and practice of low-frequency electromagnetic exploration: *Geophysics*, **13**, 584–594.
- Fraser, D. C., Keevil, N. B., Jr., and Ward, S. H., 1964, Conductivity spectra of rocks from the Craigmont ore environment: *Geophysics*, **29**, 832–847.
- Fuller, B. D., and Ward, S. H., 1970, Linear system description of the electrical properties of rocks: *Inst. Elect. Electron. Eng. Trans. Geosci. Electron.*, **GE-8**, 7–18.
- Fuller, J. A., and Wait, J. R., 1976, A pulsed dipole in the earth, *in* Felsen, L. B., Ed., *Transient electromagnetic fields*: Springer-Verlag New York, Topics in applied physics, **10**, 237–269.
- Grahame, D. C., 1952, Mathematical theory of the faradaic admittance (pseudocapacity and polarization resistance): *J. Electrochem. Soc.*, **99**, 370c–385c.
- Jaffé, G., and Rider, J. A., 1952, Polarization in electrolytic solutions, part II: Measurements: *J. Chem. Phys.*, **20**, 1077–1087.
- Keller, G. V., 1959, Analysis of some electrical transient measurements on igneous, sedimentary and metamorphic rocks, *in* Wait, J. R., Ed., *Overvoltage research and geophysical applications*: Pergamon Press, Internat. Series on Earth Sciences, **4**, 92–111.
- Keller, G. V., and Licastró, P. H., 1959, Dielectric constant and electric resistivity of natural-state cores: *U.S. Geol. Surv. Bull.*, **1052-H**, 257–285.
- Klein, J. D., and Sill, W. R., 1982, Electrical properties of artificial clay-bearing sandstones: *Geophysics*, **47**, 1593–1605.
- Klein, J. D., Biegler, T., and Horne, M. D., 1984, Mineral interfacial processes in the method of induced polarization: *Geophysics*, **49**, 1105–1114.
- Lima, O. A. L., and Sharma, M. M. A., 1992, A generalized Maxwell-Wagner theory for membrane polarization in shaly sands: *Geophysics*, **57**, 789–799.
- Madden, T. R., and Cantwell, T., 1967, Induced polarization: A review, *in* Soc. Expl. Geophys. Ed. Comm. Mining Geophys., **II**, 373–400.
- Madden, T. R., and Marshall, D. J., 1959a, Electrode and membrane polarization: MIT Report to U.S. Atomic Energy Comm., RME-3157.
- 1959b, Induced polarization, a study of its causes and magnitudes in geologic materials: MIT Final Report to U.S. Atomic Energy Comm., RME-3160.
- Mahan, M. K., Redman, J. D., and Strangway, D. W., 1986, Complex resistivity of synthetic sulphide bearing rocks: *Geophys. Prosp.*, **34**, 743–768.
- Maxwell, J. C., 1891, A treatise on electricity and magnetism, **I** (Edition 1954): Dover Publ. Inc.
- Morrison, H. F., Phillips, R. J., and O'Brien, D. P., 1969, Quantitative interpretation of transient electromagnetic fields over a layered half space: *Geophys. Prosp.*, **17**, 82–101.
- Nelson, P. H., Hansen, W. H., and Sweeney, M. J., 1982, Induced polarization response of zeolitic conglomerate and carbonaceous siltstone: *Geophysics*, **47**, 71–88.
- Olhoft, G. R., 1985, Low frequency electrical properties: *Geophysics*, **50**, 2492–2503.
- Pelton, W. H., 1977, Interpretation of complex resistivity and dielectric data: Ph.D. thesis, Univ. Utah.
- Pelton, W. H., Ward, S. H., Hallof, P. G., Sill, W. R., and Nelson, P. H., 1978, Mineral discrimination and removal of inductive coupling with multi-frequency IP: *Geophysics*, **43**, 588–609.
- Scott, J. H., Carroll, R. D., and Cunningham, D. R., 1967, Dielectric constant and electrical conductivity measurements of moist rock: A new laboratory method: *J. Geophys. Res.*, **72**, 5101–5115.
- Seigel, H. O., 1959a, A theory for induced polarization effect (for step function excitation), *in* Wait, J. R., Ed., *Overvoltage research and geophysical applications*: Pergamon Press, Internat. Series on Earth Sciences, **4**, 4–21.
- 1959b, Mathematical formulation and type curves for induced polarization: *Geophysics*, **24**, 547–565.
- Van Voorhis, G. D., Nelson, P. H., and Drake, T. L., 1973, Complex resistivity spectra of porphyry copper mineralization: *Geophysics*, **38**, 49–60.
- Wait, J. R., 1959a, A phenomenological theory of overvoltage for metallic particles, *in* Wait, J. R., Ed., *Overvoltage research and geophysical applications*: Pergamon Press, Internat. Series on Earth Sciences, **4**, 22–28.
- 1959b, The variable-frequency method, *in* Wait, J. R., Ed., *Overvoltage research and geophysical applications*: Pergamon Press, Internat. Series on Earth Sciences, **4**, 29–49.
- Ward, S. H., and Fraser, D. C., 1967, Conduction of electricity in rocks, *in* Soc. Expl. Geophys. Ed. Comm. Mining Geophys., **II**, 197–223.
- Wong, J., 1979, An electrochemical model of the induced polarization phenomena in disseminated sulphide ores: *Geophysics*, **44**, 1245–1265.
- Zonge, K. L., 1972, Electrical properties of rocks as applied to geophysical prospecting: Ph.D. thesis, Univ. Arizona.

## APPENDIX A

### INVARIANCE OF THE COMPLEX CONDUCTIVITY FUNCTION REPRESENTATION (DIAS, 1968)

Let us first make a combination of resistors in series and/or parallel with a fundamental circuit any number of times and in any sequential order. Second, let us combine an indefinite number of fundamental circuits in series and/or parallel, in any sequential order, provided these circuits are linearly dependent.

For the fundamental circuit represented in Figure 2, admittance is given by

$$\frac{1}{Z_1} = \frac{1}{R} + \frac{1}{R_1 + Z'} \quad (\text{A-1})$$

and the complex conductivity is written as

$$\sigma = \frac{c}{Z_1} = c \left( \frac{1}{R} + \frac{1}{R_1 + Z'} \right), \quad (\text{A-2})$$

where  $c$  is a geometrical factor and the frequency dependence of  $\sigma$  comes from the term containing  $Z'$ .

Let us define an operator  $R_1$  which, applied on  $Z_1$ , results in a combination of the circuit  $Z_1$  in parallel with a single arbitrary

resistor  $R'$ . Similarly, an operator  $R_2$  acting on  $Z_1$  results in a series combination of  $Z_1$  with a single arbitrary resistor  $R''$ .

For operation  $R_1(Z_1)$ , the admittance function can be written as

$$\frac{1}{Z} = \frac{1}{R'} + \frac{1}{Z_1} \quad (\text{A-3})$$

and the corresponding conductivity can be written as

$$\sigma = c_1 \left[ \left( \frac{1}{R} + \frac{1}{R'} \right) + \frac{1}{R_1 + Z'} \right]. \quad (\text{A-4})$$

From the structure of function  $\sigma$  given by equation (A-4), it is obvious that it will be formally the same as the one given by equation (A-2) as a function of frequency. Any possible difference will come in the values of the coefficients in that function.

For operation  $R_2(Z_1)$ , the admittance function is now given as

$$\frac{1}{Z} = \frac{1}{R'' + Z_1} = \frac{1}{R'' + \frac{R(R_1 + Z')}{R + R_1 + Z'}}, \quad (\text{A-5})$$

which can be rewritten as

$$\frac{1}{Z} = \frac{R + R_1 + Z'}{R''(R + R_1) + Z'(R + R'') + RR_1}, \quad (\text{A-6})$$

$$\frac{1}{Z} = \frac{R + R_1 + Z'}{(R + R'')\left(R_1 + \frac{RR''}{R+R''} + Z'\right)}, \quad (\text{A-7})$$

and

$$\frac{1}{Z} = \left(\frac{R}{R + R''}\right)^2 \left(\frac{R + R''}{R^2} + \frac{1}{R_1 + \frac{RR''}{R+R''} + Z'}\right). \quad (\text{A-8})$$

Introducing in equation (A-8) the substitution

$$a = R_1 + \frac{RR''}{R + R''} \quad (\text{A-9})$$

results in

$$\frac{1}{Z} = \left(\frac{a - R_1}{R''}\right)^2 \left(\frac{R + R''}{R^2} + \frac{1}{a + Z'}\right) \quad (\text{A-10})$$

and

$$\sigma = c \left(\frac{R''/R}{a - R_1} + \frac{1}{a + Z'}\right), \quad (\text{A-11})$$

which, as a function of frequency, is the same kind as the one obtained through equation (A-2) or (A-4).

For operations  $R_2(R_1 Z_1)$  or  $R_1(R_2 Z_1)$ , operator  $R_2$  is applied on the function resulting from  $R_1$  acting on  $Z_1$ , or vice-versa. As shown before, the operation  $R_1(Z_1)$  does not formally change the type of frequency function. The same happens for  $R_2$  applied on the resulting function. The sequential order of the two

operations is interchangeable. Therefore, any number of such operations following any sequential order should not formally change the complex conductivity as a function of frequency, but will change the values of its coefficients.

Let us define the operators  $P_1$  and  $P_2$  which, acting on two fundamental circuits, will result in combinations of these circuits in parallel and in series, respectively. We will keep the simplest case, assuming these circuits to be linearly dependent. For such a case,

$$Z'_1 = a_1 Z_1, \quad (\text{A-12})$$

where  $a_1$  is a real quantity. The values  $P_1(Z_1, Z'_1)$  and  $P_2(Z_1, Z'_1)$  correspond, respectively, to

$$\frac{1}{Z} = \frac{1}{Z_1} + \frac{1}{Z'_1} = \left(1 + \frac{1}{a_1}\right) \frac{1}{Z_1} \quad (\text{A-13})$$

and

$$\frac{1}{Z} = \frac{1}{Z_1 + Z'_1} = \left(\frac{1}{1 + a_1}\right) \frac{1}{Z_1}. \quad (\text{A-14})$$

In such a situation, it is trivial to prove the form invariance of the complex conductivity function by applying  $P_1$  and  $P_2$  any number of times in any sequential order.

The network that corresponds to a core sample of a polarizable rock can be generated through a large number of sequential applications of the operators  $R_1$ ,  $R_2$ ,  $P_1$ , and  $P_2$  on a particular fundamental circuit  $Z_1$  following a certain order. Therefore, as demonstrated, the function of frequency which describes the behavior of the fundamental circuit is like the one associated with the entire rock sample.

## APPENDIX B

### DERIVATION OF THE NEW $\sigma$ FROM THE ORIGINAL FUNCTION

The original function  $\sigma$  set by Dias (1968, 1972) is reproduced as

$$\sigma = \sigma_0 + \frac{AF(1+i)f^{1/2}}{1 + BF_1(1+i)f^{1/2}}, \quad (\text{B-1})$$

where  $f$  is the frequency in Hertz,

$$F = 1 + (C/A)f^{1/2}[1 + i + (D/C)if^{1/2}], \quad (\text{B-2})$$

and

$$F_1 = F - [D/(2AB)]f^{1/2}[1 + i + (D/C)if^{1/2}]. \quad (\text{B-3})$$

The coefficients appearing in equations (B-1) through (B-3) are related to the circuit parameters of Figure 1 as

$$1/Z = g\sigma; \quad 1/R = g\sigma_0, \quad (\text{B-4})$$

$$\pi^{1/2}/a = gA; \quad \pi C_{d\ell} = gC, \quad (\text{B-5})$$

and

$$2\pi^{3/2}rC_{d\ell}/a = gD; \quad \pi^{1/2}(r + R_s)/a = B, \quad (\text{B-6})$$

$g$  being a geometrical factor given by  $S/d$ , where  $S$  is the cross-sectional area and  $d$  is the length of the rock sample. A change in the sign of  $i$ , the imaginary unit, was introduced in the original expression of  $\sigma$  because of the time dependence representation ( $e^{i\omega t}$ ).

Let us recognize that

$$F = 1 + u \quad (\text{B-7})$$

and

$$F_1 = 1 + [1 - D/(2BC)]u, \quad (\text{B-8})$$

where

$$u = (D/A)if[1 + (C/D)(2/(if))^{1/2}]. \quad (\text{B-9})$$

The new parameters introduced in the text are related to the old ones as follows:

$$\tau = rC_{d\ell} = D/(2\pi A), \quad (\text{B-10})$$

$$\eta = a/r = 2\pi^{1/2}C/D, \quad (\text{B-11})$$

$$\delta = \frac{r}{r + R_s} = D/(2BC), \quad (\text{B-12})$$

and

$$m = \frac{R}{R + R_s} = \frac{1}{1 + R_s/R} = \frac{1}{1 + \sigma_0 \frac{B}{A} \left(1 - \frac{D}{2BC}\right)}. \quad (\text{B-13})$$

Introducing  $\omega = 2\pi f$  and the new parameters in function (B-1) normalized to  $\sigma_0$ , one can write

$$\sigma/\sigma_0 = 1 + \left( \frac{A}{\pi^{1/2}\sigma_0} \right) \frac{F(i\omega)^{1/2}}{1 + \frac{B}{\pi^{1/2}} F_1(i\omega)^{1/2}}, \quad (\text{B-14})$$

where

$$F = 1 + \mu, \quad (\text{B-15})$$

$$F_1 = 1 + (1 - \delta)\mu, \quad (\text{B-16})$$

$$\mu = i\omega\tau[1 + \eta(i\omega)^{-1/2}], \quad (\text{B-17})$$

$$\frac{A}{\pi^{1/2}\sigma_0} = [m(1 - \delta)/(1 - m)] \frac{B}{\pi^{1/2}}, \quad (\text{B-18})$$

and

$$\frac{B}{\pi^{1/2}} = (\eta\delta)^{-1}. \quad (\text{B-19})$$

So we can obtain from equation (B-14), through substitutions of equations (B-15)–(B-19), the following expression for  $\sigma$ :

$$\sigma = \sigma_0 \left[ 1 + \alpha \frac{\lambda\beta(i\omega)^{1/2}}{1 + \lambda'\beta(i\omega)^{1/2}} \right], \quad (\text{B-20})$$

where  $\lambda$ ,  $\lambda'$ ,  $\mu$ ,  $\alpha$ , and  $\beta$  are the same functions as equations (14)–(18).

## APPENDIX C

### DERIVATION OF THE COMPLEX RESISTIVITY FOR THE MODELS ASSOCIATED WITH FIGURES 2 AND 3

These models have the associated equivalent circuit analog of the type represented in Figure 2 and the relations given in Table 2. Derivation is of a general function representation.

The impedance to this system is given by

$$Z = \frac{R(R_1 + Z')}{R + R_1 + Z'}, \quad (\text{C-1})$$

with its particular values and functions given in Table 2.

For items 1–6 in Table 2 (for which  $Z' \rightarrow \infty$ , when  $\omega \rightarrow 0$ ), we start with

$$\begin{aligned} Z/Z_0 &= \frac{R_1 + Z'}{R + R_1 + Z'} = 1 - \frac{R}{R + R_1 + Z'} \\ &= 1 - \frac{R}{R + R_1} \frac{R + R_1}{R + R_1 + Z'} \end{aligned} \quad (\text{C-2})$$

and get

$$Z/Z_0 = 1 - m \left( 1 - \frac{Z'}{R + R_1 + Z'} \right) \quad (\text{C-3})$$

and

$$\rho = \rho_0 \left[ 1 - m \left( 1 - \frac{1}{1 + (R + R_1)/Z'} \right) \right]. \quad (\text{C-4})$$

The term  $(R + R_1)/Z'$  comes explicitly for each particular case in the text.

For items 7 and 8 in Table 2 (for which  $Z'$  is finite when  $\omega \rightarrow 0$ ), we start from equation (C-1) and introduce the corresponding  $Z_0$  given in Table 2, obtaining

$$Z/Z_0 = \left( 1 + \frac{R}{R_1 + Z'_0} \right) \left( \frac{R_1 + Z'}{R + R_1 + Z'} \right). \quad (\text{C-5})$$

We then go through

$$Z/Z_0 = \left( 1 + \frac{R/Z'_0}{1 + R_1/Z'_0} \right) \left( 1 - \frac{R}{R + R_1 + Z'} \right), \quad (\text{C-6})$$

$$\begin{aligned} Z/Z_0 &= 1 - \frac{R}{R + R_1 + Z'} \\ &\quad + \frac{R/Z'_0}{1 + R_1/Z'_0} \left( 1 - \frac{R}{R + R_1 + Z'} \right), \end{aligned} \quad (\text{C-7})$$

and

$$\begin{aligned} Z/Z_0 &= 1 - \frac{R}{1 + R_1/Z'_0} \left( \frac{1 + R_1/Z'_0}{R + R_1 + Z'} \right. \\ &\quad \left. - \frac{1}{Z'_0} + \frac{R/Z'_0}{R + R_1 + Z'} \right). \end{aligned} \quad (\text{C-8})$$

Let us introduce  $m$  given in Table 2, obtaining

$$\begin{aligned} Z/Z_0 &= 1 - m \frac{(R + R_1)}{R + R_1 + Z'} \left[ 1 + \frac{R + R_1}{Z'_0} \right. \\ &\quad \left. - \frac{1}{Z'_0} (R + R_1 + Z') \right], \end{aligned} \quad (\text{C-9})$$

$$Z/Z_0 = 1 - m \left( 1 - \frac{Z'}{R + R_1 + Z'} \right) \left( 1 - \frac{Z'}{Z'_0} \right), \quad (\text{C-10})$$

and

$$Z/Z_0 = 1 - m \left( 1 - \frac{1}{1 + (R + R_1)/Z'} \right) \left( 1 - \frac{Z'}{Z'_0} \right) \quad (\text{C-11})$$

to get

$$\rho = \rho_0 \left[ 1 - m \left( 1 - \frac{1}{1 + (R + R_1)/Z'} \right) \left( 1 - \frac{Z'}{Z'_0} \right) \right]. \quad (\text{C-12})$$

Expression (C-12) can be of general use for these cases. For such a purpose, it is enough to exclude the point zero from the dominion of the variable  $\omega$  when using expression (C-12), then vanishing  $Z'/Z'_0$  and  $R_1/Z'_0$  for cases 1–6 and so reducing expression (C-12) to expression (C-4).

Under the constraint set for cases 7 and 8, given by  $(R + R_1)/Z'_0 \gg 1$ , expression (C-12) is reduced to

$$\rho = \rho_0 \left[ 1 - m \left( 1 - \frac{Z'}{Z'_0} \right) \right], \quad (\text{C-13})$$

where

$$Z'/Z'_0 = \frac{1}{(1 + i\omega\tau)^c} \quad (\text{for case 7}) \quad (\text{C-14})$$

and

$$Z'/Z'_0 = \frac{1}{[1 + (i\omega\tau)^c]^k} \quad (\text{for case 8}). \quad (\text{C-15})$$

In both cases,  $\tau = 1/\omega_L$ .

For the multi-Cole-Cole model, having the associated equivalent circuit analog represented in Figure 3, the impedance associated to this system is given by

$$Z = \frac{Z_1 Z_2}{Z_1 + Z_2}, \quad (\text{C-16})$$

where

$$Z_1 = \frac{R'(R_1 + Z'_1)}{R' + R_1 + Z'_1} \quad \text{and} \quad Z_2 = \frac{R''(R_2 + Z'_2)}{R'' + R_2 + Z'_2}. \quad (\text{C-17})$$

When  $\omega \rightarrow 0$ , one obtains

$$Z_{1,0} = R'; \quad Z_{2,0} = R'' \quad \text{and} \quad Z_0 = \frac{R'R''}{R' + R''}. \quad (\text{C-18})$$

By introducing the parameters

$$m_1 = \frac{R'}{R_1 + R'} \quad \text{and} \quad \tau_1 = \left( \frac{R_1 + R'}{a_1} \right)^{1/c_1} \quad (\text{C-19})$$

and

$$m_2 = \frac{R''}{R_2 + R''} \quad \text{and} \quad \tau_2 = \left( \frac{R_2 + R''}{a_2} \right)^{1/c_2}, \quad (\text{C-20})$$

one can write the expressions (C-17), already seen before, as

$$Z_1 = R' \left[ 1 - m_1 \left( 1 - \frac{1}{1 + (i\omega\tau_1)^{c_1}} \right) \right] \quad (\text{C-21})$$

and

$$Z_2 = R'' \left[ 1 - m_2 \left( 1 - \frac{1}{1 + (i\omega\tau_2)^{c_2}} \right) \right]. \quad (\text{C-22})$$

Since

$$Z_1 Z_2 = R'R'' \left[ 1 - m_1 \left( 1 - \frac{1}{1 + (i\omega\tau_1)^{c_1}} \right) \right] \times \left[ 1 - m_2 \left( 1 - \frac{1}{1 + (i\omega\tau_2)^{c_2}} \right) \right] \quad (\text{C-23})$$

and

$$Z_1 + Z_2 = R' + R'' - m_1 R' \left( 1 - \frac{1}{1 + (i\omega\tau_1)^{c_1}} \right) - m_2 R'' \left( 1 - \frac{1}{1 + (i\omega\tau_2)^{c_2}} \right), \quad (\text{C-24})$$

equation (C-16) becomes

$$Z = \left( \frac{R'R''}{R' + R''} \right) \frac{1}{D} \left[ 1 - m_1 \left( 1 - \frac{1}{1 + (i\omega\tau_1)^{c_1}} \right) \right] \times \left[ 1 - m_2 \left( 1 - \frac{1}{1 + (i\omega\tau_2)^{c_2}} \right) \right], \quad (\text{C-25})$$

where

$$D = 1 - \left( \frac{1}{1 + R_1/R'} \right) \left( \frac{1}{1 + R''/R'} \right) \left( 1 - \frac{1}{1 + (i\omega\tau_1)^{c_1}} \right) - \left( \frac{1}{1 + R_2/R''} \right) \left( \frac{1}{1 + R'/R''} \right) \left( 1 - \frac{1}{1 + (i\omega\tau_2)^{c_2}} \right). \quad (\text{C-26})$$

By substituting  $Z_0$  in equation (C-25), given in equation (C-18), one obtains

$$Z/Z_0 = \frac{1}{D} \left[ 1 - m_1 \left( 1 - \frac{1}{1 + (i\omega\tau_1)^{c_1}} \right) \right] \times \left[ 1 - m_2 \left( 1 - \frac{1}{1 + (i\omega\tau_2)^{c_2}} \right) \right]. \quad (\text{C-27})$$

Supposing at least one of the following three conditions [(1)  $R_1 \gg R' \gg R''$ , (2)  $R_2 \gg R'' \gg R'$ , or (3)  $R_1 \gg R'$  and  $R_2 \gg R''$ ] is satisfied, we have  $D \simeq 1$ . We can finally write

$$\rho = \rho_0 \left[ 1 - m_1 \left( 1 - \frac{1}{1 + (i\omega\tau_1)^{c_1}} \right) \right] \times \left[ 1 - m_2 \left( 1 - \frac{1}{1 + (i\omega\tau_2)^{c_2}} \right) \right]. \quad (\text{C-28})$$